Received: 23 April 2021 | Revised: 16 June 2021 | Accepted: 21 June 2021

DOI: 10.1096/fj.202100686R

RESEARCH ARTICLE

THE FASEB JOURNAL

# Elucidating the structure and functions of Resolvin D6 isomers on nerve regeneration with a distinctive trigeminal transcriptome

**Thang L. Pham**[1] | **Azucena H. Kakazu**[1] | **Jiucheng He**[1] | **Robert Nshimiyimana**[2] | **Nicos A. Petasis**[2] | **Bokkyoo Jun**[1] | **Nicolas G. Bazan**[1] | **Haydee E. P. Bazan**[1]

[1]Neuroscience Center of Excellence, School of Medicine, Louisiana State University Health New Orleans, New Orleans, LA, USA

[2]Department of Chemistry and Loker Hydrocarbon Research Institute, University of Southern California, Los Angeles, CA, USA

**Correspondence**
Haydee E. P. Bazan, Neuroscience Center of Excellence, School of Medicine, Louisiana State University Health New Orleans, 2020 Gravier St., Ste. D, New Orleans, LA 70112-2223, USA.
Email: hbazan1@lsuhsc.edu

**Funding information**
National Institutes of Health, Grant/Award Number: R01EY019465; National Eye Institute

## Abstract

Innervation sustains cornea integrity. Pigment epithelium-derived factor (PEDF) plus docosahexaenoic acid (DHA) regenerated damaged nerves by stimulating the synthesis of a new stereoisomer of Resolvin D6 (RvD6si). Here, we resolved the structure of this lipid isolated from mouse tears after injured corneas were treated with PEDF + DHA. RvD6si synthesis was inhibited by fluvoxamine, a cytochrome P450 inhibitor, but not by 15- or 5-LOX inhibitors, suggesting that the 4- and 17-hydroxy of DHA have an *RR*- or *SR*-configuration. The two compounds were chemically synthesized. Using chiral phase HPLC, four peaks of RvD6si$_{1\text{-}4}$ from tears were resolved. The *RR*-RvD6 standard eluted as a single peak with RvD6$_1$ while pure *SR*-RvD6 eluted with RvD6$_3$. The addition of these pure mediators prompted a trigeminal ganglion transcriptome response in injured corneas and showed that *RR*-RvD6 was the more potent, increasing cornea sensitivity and nerve regeneration. *RR*-RvD6 stimulates *Rictor* and hepatocyte growth factor (*hgf*) genes specifically as upstream regulators and a gene network involved in axon growth and suppression of neuropathic pain, indicating a novel function of this lipid mediator to maintain cornea integrity and homeostasis after injury.

**KEYWORDS**

corneal nerves, hgf, pain, Rictor, RvD6 stereoisomers, trigeminal ganglia transcriptome

## 1 | INTRODUCTION

High-dense corneal innervation is essential to ocular surface integrity,[1] and nerve damage impairs tear production, blinking reflex, and epithelial wound healing that results in the loss of transparency and vision.[2-5] Anatomically, the axons from sensory nerves derived from the ophthalmic branch of the trigeminal ganglion (TG) neurons penetrate the corneal stroma from the limbal area and branch out as the subepithelial nerve network before terminating as free nerve endings in the superficial corneal epithelia.[6]

Factors that can alter corneal innervation include aging, diabetes, and viral and bacterial infections. Moreover, nerve damage also occurs after refractive surgery, such as

**Abbreviations:** DHA, docosahexaenoic acid; HGF, hepatocyte growth factor; PEDF, pigment epithelial-derived factor; Rictor, Rapamycin-insensitive companion of mammalian target of rapamycin; RvD6si, Resolvin D6 stereoisomers; SP, substance P; TG, trigeminal ganglion.

laser-assisted in-situ keratomileusis (LASIK) and photorefractive keratectomy,[7-9] and it takes between 3 and 15 years to recover the integrity of corneal nerves.[7,10] Consequently, corneal sensitivity decreases and dry-eye disease can develop, causing neuropathic pain, corneal ulcers, and in severe cases, corneal transplant[11-13] new therapeutic approaches are needed for treating these complications.

Previous studies from our laboratory have demonstrated that pigment epithelium-derived factor (PEDF), a glycosylated neurotrophic protein, in combination with docosahexaenoic acid (DHA), a member of the ω-3 fatty acid family, play an important role in regenerating the corneal nerves after damage and in maintaining a healthy cornea.[14,15] We have successfully tested the action of PEDF + DHA in corneas after experimental surgery and pathologies such as diabetes and herpes simplex virus (HSV1) infection.[16-20] Recently, a novel Resolvin D6-stereospecific isomer (named RvD6si) was discovered as the main pro-resolving lipid mediator underlying the mechanism of PEDF + DHA.[21] The new lipid stimulates a specific transcriptome in the TG, increasing the induction of genes related to axon growth and modulating genes involved in neuropathic pain.[21] Even though RvD6si (4,17-di-hydroxy-DHA) from tears was characterized by LC-MS/MS and its biological activity evaluated by in vivo studies, the lack of a defined stereo structure is a big factor to establish the possible therapeutic use to recover ocular surface health and integrity. This study focused on investigating the configuration of the two hydroxy groups of the RvD6si as well as the biological activities on corneal nerve regeneration after an experimental injury that mimics the nerve damage after refractive surgery. The action of the chemically synthesized pure isomers on the TG transcriptome was also investigated.

## 2 | MATERIALS AND METHODS

### 2.1 | Animals

Nine-week-old male CD1 mice were purchased from Charles River (Wilmington, MA, USA) and maintained in a 12-hours dark/light cycle at the Neuroscience Center of Excellence animal care facility, Louisiana State University Health New Orleans, LA. The animals were handled following the guidelines of the Association for Research in Vision and Ophthalmology Statement for the Use of Animals in Ophthalmic and Vision Research, and the experimental protocols were approved by the Institutional Animal Care and Use Committee at Louisiana State University Health New Orleans.

### 2.2 | Corneal injury and collection of tears

Mice were anesthetized using intraperitoneal injection of ketamine (200 mg/kg) and xylazine (10 mg/kg) and topically anesthetized using one drop of proparacaine hydrochloride solution (0.5%). The center of the cornea of the right eye was demarcated with a 2 mm trephine, and the epithelium and 1/3 of the anterior stroma were gently removed under a surgical microscope with a corneal rust ring remover (Algerbrush II; Alger Equipment Co., Lago Vista, TX, USA), as described previously.[20,21] To prevent postoperative infection, 0.3% of tobramycin ophthalmic solution (Henry Schein, Melville, NY, USA) was topically applied to the eye. For consistency, only one investigator (JH) performed all surgeries. For the tears collection, injured mice were treated topically with 10 μL of a mixture of PEDF (0.5 μg/mL) and DHA (50 nM) every 30 minutes for 4 hours after injury, and tears were collected in 1 mL of MeOH as described[21] and stored at −80°C until used.

### 2.3 | Corneal organ culture and inhibitors treatment

Twenty-four hours after injury, 50 mice were euthanized, and the eyes were enucleated. The corneas were excised and kept in ice-cold PBS. Each cornea was placed in a single well of a 48-well plate. A volume of 100 μL of DMEM medium containing inhibitors described in Table 1 was added to cover the entire cornea and incubated for 1 hour. Then, 100 μL of medium with the inhibitors and containing PEDF (50 ng/mL) + DHA (300 nM) was added, and the corneas were incubated for an additional 4 hours. Afterward, 2 mL of media (from 10 corneas) was collected and centrifuged at 19 000 *g* for 15 minutes at 4℃ to remove cellular debris. The supernatant was collected and subjected to lipid extraction.

**TABLE 1** Characteristics of the enzymes inhibitors

| Target name | Inhibitor/ abs name | Company—Cat# | Conc. | Effect |
|---|---|---|---|---|
| P450 (CYP1A2) | Fluvoxamine | Cayman chemical—15617 | 100 nM | Good |
| 15-LOX | ML351 | Cayman chemical—16119 | 200 nM | None |
| 5-LOX | Zileuton | Cayman chemical—10006967 | 60 μM | None |
| 5-LOX Abs | Mono-Rb | Abcam—ab169755 | 10 μg/mL | None |

## 2.4 | Lipid extraction and LC-MS/MS-based lipidomic analysis

Lipids from organ culture experiments were extracted by the Blight and Dyer method.[22] Briefly, 3.75 mL of a mixture of $CHCl_3$: MeOH (1:2) was added to 2 mL of sample and 5 μL of the deuterium-labeled internal standard mixture of lipids [AA-d8 (5 ng/μL), PGD-d4 (1 ng/μL), EPA-d5 (1 ng/μL), and LTB4-d4 (1 μg/μL)]. The samples were vortexed and stored at −80°C overnight. The next day, to make two phases, 2.5 mL of $CHCl_3$ was added, vortexed, followed by the addition of 2.5 mL of water (pH 3.5), vortexed, and the pH of the upper phase was adjusted to 3.5-4.0 with 1 N HCl. The lower phase was collected, dried under N2, resuspended in 1 mL of MeOH, and stored at −80°C until used. Lipids from tears of the injured mice were collected and extracted as described previously.[21] Briefly, 5 μL of sterile PBS was applied in the inferior cul-de-sac of the mouse eye for 30 seconds before the tears were collected with a 10 μL pipette in 1 mL of ice-cold MeOH, followed by the addition of 2 mL of $CHCl_3$ and 5 μL of an internal standard mixture of deuterium-labeled lipids. The samples were stored at −80°C overnight, and the lipids were extracted the following day.

For LC-MS/MS analysis, a Xevo TQ equipped with Acquity I class ultra-performance liquid chromatography (UPLC) with a flow-through needle (Waters Corporation, Milford, MA, USA) was employed as described previously.[15,21] Briefly, samples were dried under N2, resuspended in 20 μL of MeOH/$H_2O$ (2:1), and injected into a CORTECS C18 2.7 μm 4.6 × 100 mm column (Water, MA, USA). The column temperature was set at 45°C with a flow of 0.6 mL/min. The initial mobile phase consisted of 45% solvent A ($H_2O$ + 0.01% acetic acid) and 55% solvent B (MeOH + 0.01% acetic acid) and then a gradient to 15% solvent A for the first 10 minutes followed by a gradient to 2% solvent A for 18 minutes, 2% solvent A run isocratically until 25 minutes, and then a gradient back to 45% solvent A for re-equilibration until 30 minutes.

For the spike-in experiments, isolated RvD6si from tears was mixed with chemically synthetized RR-RvD6 or SR-RvD6 at the same molarity. The samples were dried under N2, resuspended in 20 μL of MeOH/$H_2O$ (2:1), and injected into a CHIRALPAK AD-RH column (Chiral Technologies, Inc, PA, USA). The column temperature was set at 45°C with a flow of 0.6 mL/min. The initial mobile phase consisted of 60% solvent A ($H_2O$ + 0.01% acetic acid) and 40% solvent B (acetonitrile +0.01% acetic acid) and then a gradient to 10% solvent A for the first 15 minutes, followed by 10 minutes of 100% solvent B and then a gradient back to 60% solvent A for re-equilibration until 30 minutes.

Lipid standards (Cayman, Ann Arbor, MI, USA) were used for tuning and optimization. SS-RvD6 standard, [4*S*,17*S*-dihydroxy-5*E*,7*Z*,10*Z*,13*Z*,15*E*,19*Z*-docosahexaenoic acid] was a generous gift of Dr Charles Serhan (Harvard University, Boston, MA, USA).

## 2.5 | In vivo treatments

After corneal injury, mice were randomly divided into four groups (8-10 animals per group) and treated topically with 10 μL of RR-RvD6 or SR-RvD6 at the concentration of 1 ng/μL three times per day for 12 days. The lipids dissolved in ethanol were aliquoted for each day's treatment and stored at −80°C. Before treatment, the ethanol was evaporated under $N_2$, and the lipids were resuspended in PBS. Vehicle (ethanol evaporated and PBS) was used as the negative control, and PEDF + DHA was used as the positive control. The experiments were double-blinded.

## 2.6 | Measurement of corneal sensitivity

For this study, we used the Belmonte non-contact corneal esthesiometer[23] that is a more reliable method than the standard Cochet-Bonnet esthesiometer to determine the corneal sensation threshold,[24] as described previously.[21] Sensitivity was measured in the holding mice with an air output needle at 3 mm from the cornea and a starting airflow rate of 80 mL per minute. When the mouse blinked, the airflow rate was recorded as the final corneal sensitivity index. As a baseline, sensitivity was measured in each mouse before injury.

## 2.7 | Analysis of corneal nerves

Twelve days after injury and treatment, mice were euthanized, corneas obtained, and whole mounts processed, as described previously.[25] The primary antibodies used were: rabbit monoclonal anti-PGP9.5 (1:500, which is equivalent to 0.22 μg/mL) (ab108986; Abcam, Cambridge, MA, USA), and rat monoclonal anti-substance-P (SP; 1:100, which is equivalent to 1 μg/mL) (sc-21715; Santa Cruz Biotechnology, Dallas, TX, USA). The corresponding secondary antibodies were goat anti-rabbit Alexa Fluor 488 (1:1000, which is equivalent to 2 μg/mL) and goat anti-rat Alexa Fluor 488 (1:1000, which is equivalent to 2 μg/mL) (Thermo Fisher Scientific, Waltham, MA, USA). Corneas were examined with a fluorescent microscope (Deconvolution microscope DP80; Olympus, Tokyo, Japan), and nerve density was measured using the brush tool in Photoshop CC 2014 (Adobe), as described previously.[25-28]

## 2.8 | Transcriptome of trigeminal ganglion

At day 12 after injury, mice were euthanized, and the ipsilateral TG from the injury eye side of corneas treated with vehicle, *RR*-, *SR*-, or *SS*-RvD6 were collected and homogenized in 1 mL of TRIzol on ice. Total mRNA from a

single TG in each condition was obtained using an RNeasy mini kit (Qiagen, Germantown, MD, USA), as described by the manufacturer. RNA purity and concentration were determined with a NanoDrop ND-1000 spectrophotometer (Thermo Fisher Scientific), and the samples were stored at −80°C until used. RNA sequencing was performed as described previously[21] using the adapted Smart-seq2 protocol.[29] Briefly, 10 ng of total RNA was reverse transcribed using the Oligo-dT30VN and template-switching oligo (TSO) primers. The total cDNAs were amplified employing ISPCR primers, and the library was constructed with a Nextera XT DNA library preparation kit (Illumina, San Diego, CA, USA). The libraries were pooled together at the same molarity concentration and sequenced using the NextSeq 500/550 High Output Kit v2 (75 cycles, Illumina). After demultiplexing, RNA-seq data were aligned to the GENCODE GRCm38 mouse primary genome assembly (Release M22, gencodegenes.org/mouse/) using the RSubread package v1.34.6 for R v3.6.1.[30] The out-putted BAM files for sequencing data alignment were counted using the featureCounts function (Subread v1.6.5 in Ubuntu LTS 16.4 operating system).[31] The data were then subjected to differential gene expression analysis using DESeq2 package for R.[32] The adjusted *p* values were regarded as false discovery rate (FDR). Significantly changed genes (FDR < .05) between RR-RvD6 vs vehicle, SR-RvD6 vs vehicle, and SS-RvD6 vs vehicle were subjected to enrichment analysis using Enrichr[33] and pathway analysis using IPA (QIAGEN Inc, https://www.qiagenbioinformatics.com/products/ingenuity-pathway-analysis).

## 2.9 | Statistical analysis

To calculate the subbasal nerve density, the fluorescent images were changed to grayscale mode and placed against a white background using imaging software (Photoshop, Adobe System, Inc, Mountain View, CA, USA). Each image was carefully drawn with a 4-pixel line following the course of each fiber using the brush tool in the imaging software. The nerve area and the total area of the image were obtained using the histogram tool. The percentage of total nerve area was quantified for each image, as described previously.[2,6,25] Data expressed as mean ± SD of ≥3 independent experiments were analyzed by one-way ANOVA followed by Tukey's honest significant difference post hoc test at 95% confidence level to compare the different groups and considered significant when $P < .05$. All statistical and graphs were done using Prism 7 software (GraphPad Software, La Jolla, CA, USA) and BioVinci (BioTuring, La Jolla, CA, USA). For the sequencing data, the normalized counts from DE-Seq2 were used as the input of the ANOVA test.

# 3 | RESULTS

## 3.1 | Cytochrome P450 is involved in the synthesis of RvD6 isomers

Our recent study has shown that RvD6si release from tears of injured mice treated with PEDF + DHA when separated by LC-MS/MS eluted earlier than the LTB4-d4 and RvD6 standard (Figure 1A). Differences in the biological activities of these two molecules were also demonstrated.[21] Therefore, it was important to elucidate the structure of this new isomer derived from the treatment with PEDF + DHA. It has been shown that the standard RvD6, [4*S*-17*S*-dihydroxy-DHA], is generated from DHA by the action of a 15-lipoxygenase (15-LOX) followed by a 5-LOX which forms the 17S-OH and 4S-OH configurations, respectively (Figure 1B). However, DHA could also be catalyzed by the P450 cytochrome system, which forms the 17*R*-monohydroxy-DHA.[34,35] As a result, there are four possible stereo configurations for the hydroxy groups in the same 4,17-dihydro-DHA backbone (Figure 1B). In injured corneas previously incubated with inhibitors of the enzymes and then stimulated with PEDF + DHA, we found that fluvoxamine, an inhibitor of the cytochrome P450, consistently decreases the synthesis of RvD6si. Although the inhibition is 30%, the reduction is significant at a 95% of confidence level (Figure 1C). Since inhibitors and antibodies of 15-LOX and 5-LOX had no effect on RvD6si synthesis, we hypothesized that the RvD6si could be 4*R*-17*R*-dihydroxy-DHA or 4*S*-17*R*-dihydroxy-DHA. To further investigate the structure of this lipid, the total synthesis of these two lipids, RR-RvD6 and SR-RvD6, was conducted.

## 3.2 | RvD6 stereoisomer structures were confirmed by total chemical synthesis

The scheme of 4*R*-17*R*-dihydroxy-DHA synthesis is shown in Figure 2A. Briefly, the synthesis began with small and defined starting materials of known configurations, with the carbon atoms of a C1-C13 fragment. The (R) alcohol chirality at C-4 position was unambiguously confirmed and was retained from enantiomerically pure (*R*)-γ-carboxy-γ-butyrolactone, a commercially available building block. The C14-C22 fragment was built from *cis*-4-Heptenal, via an organocatalytic α-oxidation to establish the C-17 *R*-configuration with excellent enantiomeric excess. With both the C1-C13 and C14-C22 main intermediates at hand, a *Z*-stereoselective Wittig condensation between the aldehyde and ylide derivative of C1-C13 yielded the docosahexaenoate carbon skeleton of the desired compound in the methyl ester form. Further manipulations and purification were done by reversed-phase HPLC on a Phenomenex Luna® column 5 μm C18 100 Å 250 × 10 mm, 240 nm, 70% MeOH (B)/

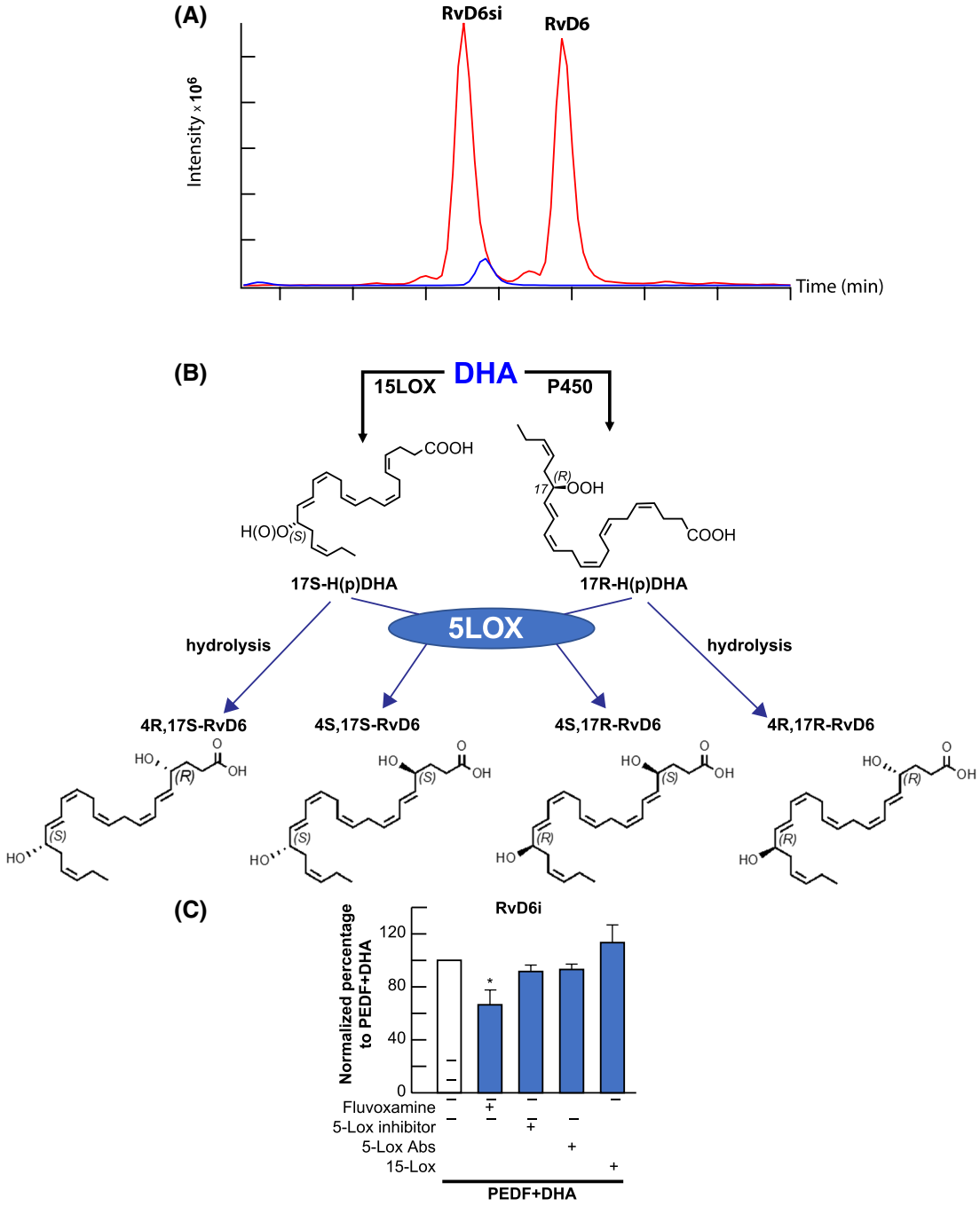


**FIGURE 1** Effect of inhibitors on RvD6si synthesis. A, Different retention time of standard RvD6 (SS-RvD6) and the RvD6si isomer isolated from tears of PEDF + DHA-treated mice. The blue peak represents the internal standard $LTB_4$-d4. The RvD6si eluted earlier than $LTB_4$-d4 and RvD6 standard. B, Possible stereoisomers of RvD6 made from DHA. The 15-LOX derivatives of RvD6 (left panel) contain the 17*S*-OH, while the P450 derivatives (right panel) contain the 17*R*-OH on the DHA backbone. 5-LOX catalyzes the formation of 4*S*-OH, while the 4*R*-OH might be formed by hydrolysis. C, Incubating corneas with inhibitors/antibodies in the presence of PEDF + DHA shows that only the cytochrome P450 inhibitor Fluvoxamine, significantly reduced the synthesis of RvD6si while 15- and 5-LOX inhibitors/antibodies had no effect. Details about inhibitors and antibodies used are described in Table 1. Values are mean ± SD * $P < .05$ using Student's *t* test with PEDF + DHA group as reference. There were 10 corneas/sample per experiment (total 50 corneas for 5 groups of treatment). An average of three independent experiments was calculated

$H_2O$ (A) to 100% (B) for 20 minutes afforded stereochemically pure *RR*-RvD6i, namely 4(*R*),17(*R*)-dihydroxydocosa-5*E*,7*Z*,10*Z*,13*Z*,15*E*,19*Z*-hexaenoic acid. The LC/MS showed a great purity (Figure 2B, left). The synthesized product also gave an ultraviolet (UV) chromophore profile with a broad-band of absorption, λmax MeOH, at ~240 nm, characteristic of conjugated 1,3-butadiene moieties present in the molecule at carbon positions C5-C7 and C13-C15.

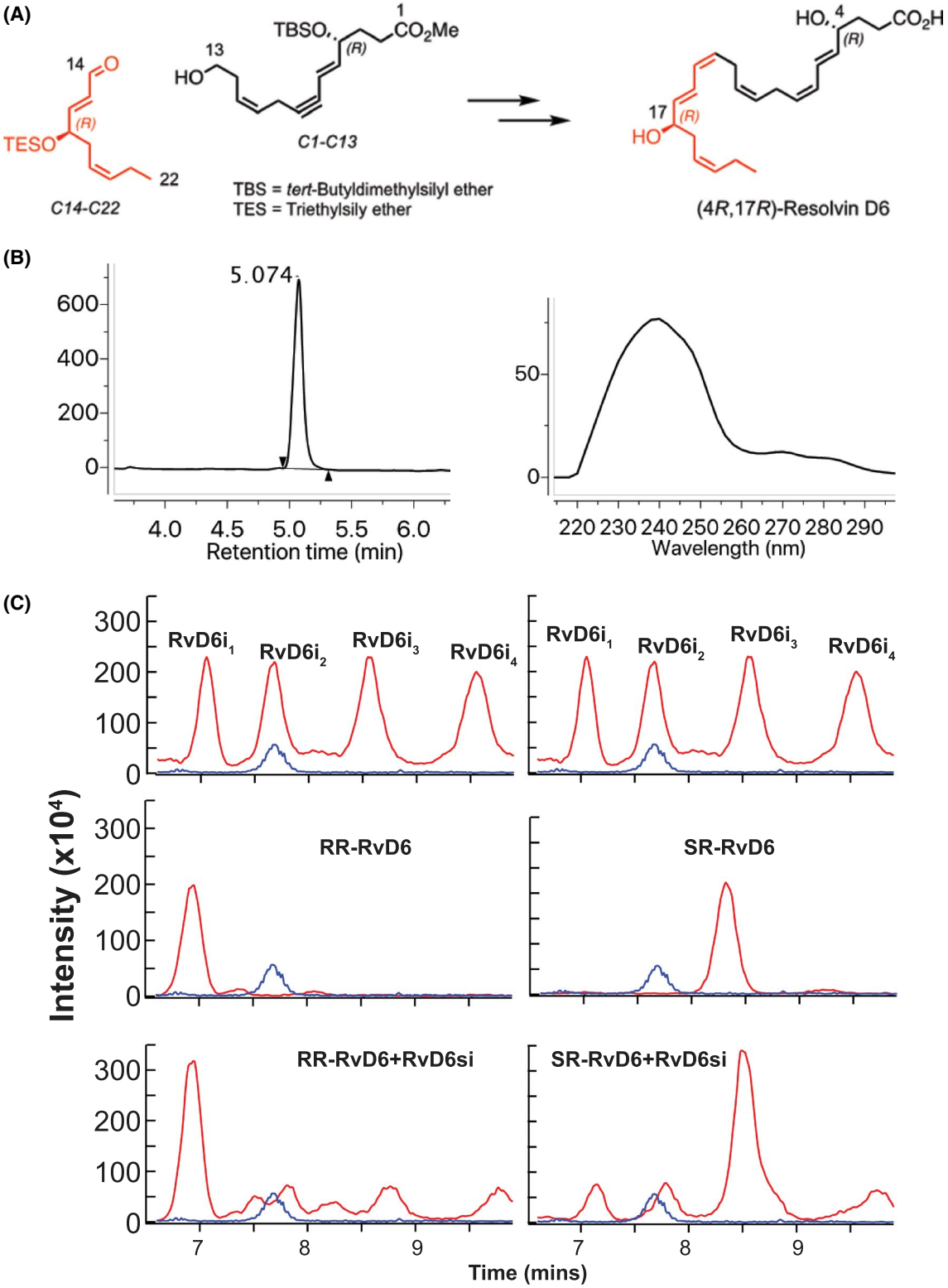


**FIGURE 2** The structure of RvD6si was confirmed by total synthesis. A, The synthetic scheme of RR-RvD6 involved key synthetic intermediates C1-C13 (black) and C14-C22 (red) were constructed from chirally pure building blocks that were synthesized in conjunction with stereospecific transformations to furnish the target with absolute stereo- and regiochemical control. B. The purity of RR-RvD6 was confirmed by LC-MS chromatogram (left) while its characteristic conjugated 1,3-butadiene moieties are shown in the molecule at carbon positions C5-C7 and C13-C15, confirmed by UV spectrum (right). B, LC-MS/MS analysis of mouse tears-derived RvD6si using a chiral column shows the separation of four peaks. Chemical synthetized RR-RvD6 had the same retention time as the first peak of RvD6si, while the SR-RvD6 partially matched the third peak of RvD6 isomer. Only RR-RvD6 has an earlier retention time than the internal standard $LTB_4$-d4 (blue), as shown in Figure 1A

To distinguish the stereoisomer structure of the RvD6si, a chiral column was used that provided enantiomer separation. Surprisingly, we found that our RvD6si isolated from mouse tears is composed of four different stereoisomers (Figure 2C) named RvD6i$_{1\text{-}4}$. Among those, the retention time of RvD6i$_1$ matched the retention time of the synthesized 4*R*-17*R*-dihydroxy-DHA (RR-RvD6) while RvD6i$_3$ partially matched the 4*S*-17*R*-dihydroxy-DHA (SR-RvD6) (Figure 2C). These two chemical synthesized lipids generate the same peaks in a spike-in experiment in which we mixed the standards with RvD6si isolated from mouse tears. Aside from the unidentified RvD6i$_2$ and RvD6i$_4$, our data show that the RvD6si we have recently reported[21] contains a 4*R*-17*R*- and a 4*S*-17*R*-dihydroxy-DHA.

## 3.3 | Biological activities of RvD6 stereoisomers on corneal nerve regeneration

For these experiments, we treated the mouse injured corneas with pure RR-RvD6 or SR-RvD6 (10 ng/eye, three times per day) for 12 days. The PEDF + DHA-treated group was used as positive control, while the vehicle-treated group was the negative control (Figure 3A). Corneal sensitivity shows a significant increase at day 3 after injury only with RR-RvD6 treatment (Figure 3B). The corneal sensitivity was 87 ± 10% in the *RR*-RvD6-treated corneas while the vehicle was 61 ± 8 ($P$ + 0.0015). This early effect is similar to our reported data for the RvD6si isolated from mouse tears.[21] Interestingly, when we look to the sensation of single mouse in each group, there were 50% (4/total of 8) mice that had more than 90% of sensitivity recovery at day 3, while the percentage of recovery with SR-RvD6, PEDF+DHA, and vehicle treatments were 25% (2/8), 22% (2/9), and 0% (0/9), respectively. On day 6, all mice in the RR-RvD6-treated group recovered their corneal sensation (Figure 3B). This robustness made the RR-RvD6-treated group significantly different to vehicle as well as to PEDF+DHA-treated corneas. SR-RvD6 also showed a higher score of corneal sensitivity recovery than vehicle. By day 9, all treated groups had a significant increase in sensitivity with respect to the vehicle-treated mice.

Corneal nerve regeneration was evaluated at 12 days after injury. Whole-mount staining of corneal total nerves (PGP 9.5 positive) (Figure 3E,C) and SP-positive nerves (Figure 3F,D) showed that mice treated with RR-RvD6 had the highest corneal nerve density of the two stereoisomers-treated mice compared to vehicle, and higher significance than the mice treated with PEDF + DHA. The percentage of total corneal nerve regeneration in the RR-RvD6-treated corneas was 75.5 ± 11.3, followed by 61.4 ± 6.8, 61 ± 13.4, and 46.9 ± 6.5% in PEDF + DHA, SR-RvD6, and vehicle, respectively. Similar results were found with substance P (SP)-positive nerves.

## 3.4 | Distinctive transcriptome in the TG after RvD6 stereoisomers treatment

Using RNA-seq analysis, we investigate the effect of RR-, SR-, and SS-RvD6 isomers in the transcriptome of the TG at day 12 after corneal injury and treatment. Our previous studies have shown that expression of genes related to neuropathic pain was modulated in the TG of mice treated with the RvD6si isolated from tears.[21] Analyzing these genes, we found that expression of tachykinin 1 (*Tac1*) that encodes SP and calcitonin-related peptide alpha (*Calca*) and calcitonin-related peptide beta (*Calcb*), both encoding calcitonin gene-related peptide (CGRP), decrease by treatment with the three lipid isomers (Figure 4A). Interestingly, the gene expression of transient receptor potential melastatin 8 (*Trpm8*), which encodes the TRPM8 ion channel expressed in sensory neurons and contributes to decrease neuropathic pain,[36,37] was activated by the two new synthetic standards RR-RvD6 and SR-RvD6 but not by SS-RvD6. This result might explain why SS-RvD6 showed a slower corneal nerve regeneration with significant recovery of corneal sensation found at day 9 after injury, as we reported previously.[21]

Our early studies using the RvD6si isolated from mice tears had demonstrated that *Rictor,* a gene that encodes the rapamycin-insensitive complex 2 for mTOR, was involved in corneal nerve regeneration.[21] Increased gene expression of this upstream regulator was found in all treated mice except for those treated with SS-RvD6 (Figure 4B). We also determined *Rictor* upregulated and downregulated genes (Figure 4C), and the IPA activation *z*-score of this transcription factor predicts that RR-RvD6 and SR-RvD6 are modulators of many of these genes (Figure 4C). In the prediction, there are about 5 of the 9 *Rictor* genes upregulated in the TG (red) that their induction was increased when corneas were treated with the SR-and RR-RvD6 compared to vehicle, and there were 36 of the 38 downregulated genes by *Rictor* (blue) that were inhibited by RR and SR-RvD6 respect to vehicle. KEGG pathway enrichment analysis of these 38 downregulated genes shows that they were mainly found in degenerative diseases such as Parkinson's disease, Alzheimer's disease, and Huntington's disease (Figure 4D).

Next, we investigated the potential effect of RR-RvD6 on biological systems using its specific changed genes list obtained by RNA-seq. The IPA Bio Functions tool predicts that most of the biological functions upregulated by RR-RvD6 in the TG belong to neuronal and axonal growth with 12 significant increase biological functions (Figure 5A). A graphic summary of the action of RR-RvD6 shows that the core of its action in the TG is hepatocyte growth factor (*hgf*) that affect functions related to cellular skeleton components and microtubule dynamics, which in turn can increase neuronal branching, quantity, and density of sensory neurons (Figure 5B). We found a significant increase in the

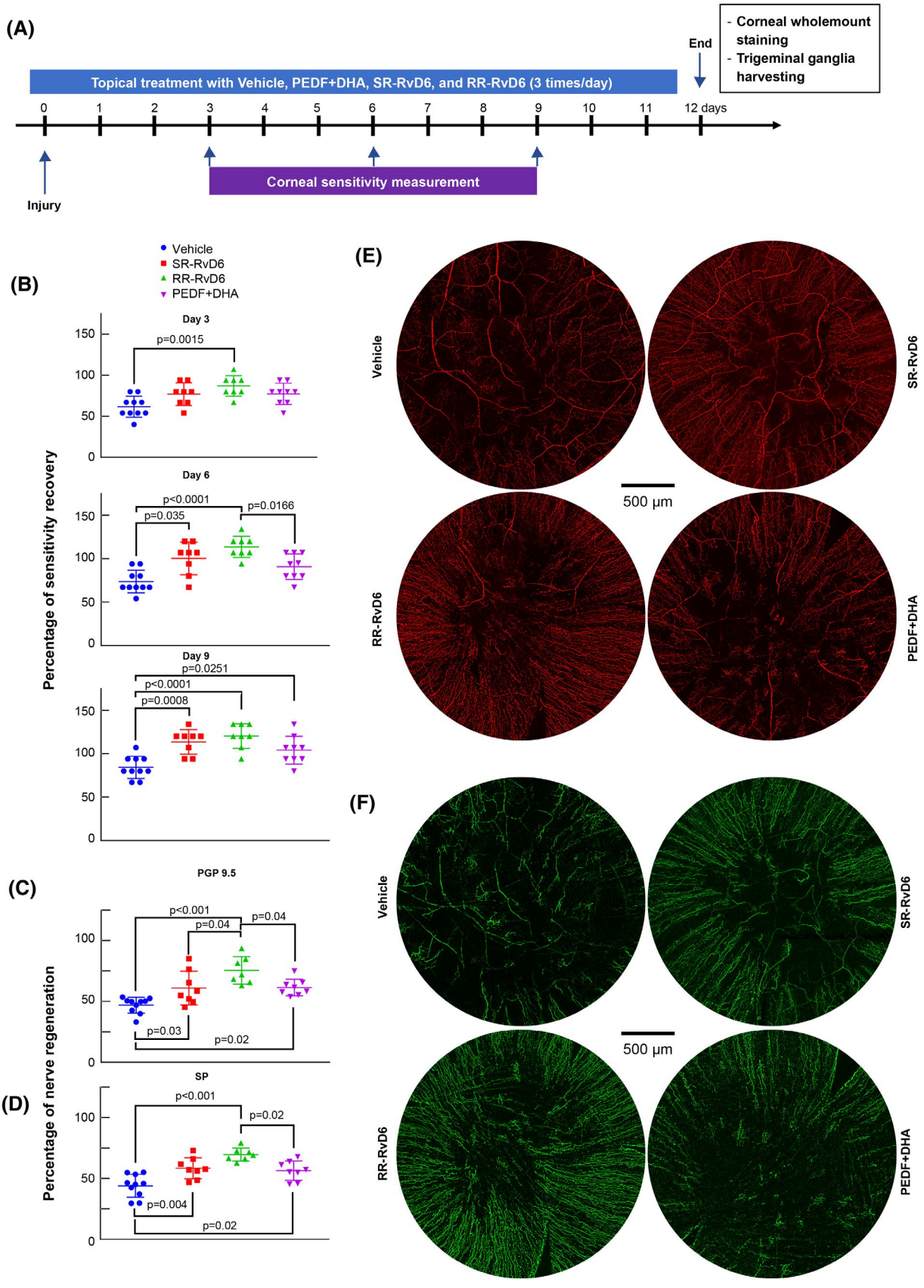
(A)
Topical treatment with Vehicle, PEDF+DHA, SR-RvD6, and RR-RvD6 (3 times/day)
End
- Corneal wholemount staining
- Trigeminal ganglia harvesting
0 1 2 3 4 5 6 7 8 9 10 11 12 days
Injury
Corneal sensitivity measurement
(B)
Vehicle
SR-RvD6
RR-RvD6
PEDF+DHA
Day 3
p=0.0015
Day 6
p<0.0001
p=0.035
p=0.0166
Day 9
p=0.0251
p<0.0001
p=0.0008
Percentage of sensitivity recovery
(C)
PGP 9.5
p<0.001
p=0.04
p=0.04
p=0.03
p=0.02
(D)
SP
p<0.001
p=0.02
p=0.004
p=0.02
Percentage of nerve regeneration
(E)
Vehicle
SR-RvD6
RR-RvD6
PEDF+DHA
500 μm
(F)
Vehicle
SR-RvD6
RR-RvD6
PEDF+DHA
500 μm

**FIGURE 3** Sensitivity and corneal nerve regeneration by the two RvD6 isomers. A, Experimental design to determine the biological activities of pure RR-RvD6 and SR-RvD6. The vehicle was used as negative control while the PEDF + DHA was used as positive reference. B, Corneal sensitivity was recorded with a non-contact corneal esthesiometer every 3 days after injury. RR-RvD6-treated mice show faster sensation recovery at day 3, followed by SR-RvD6 at day 6, and PEDF + DHA at day 9 after injury and treatment. The vehicle is used as comparative reference. Nerve density and representative whole-mount images of PGP 9.5 (C, E) and SP (D, F) positive axons at 12 days after injury and treatment. All data were normalized to the baseline (uninjured corneas) as 100%. The *p* values were calculated by one-way ANOVA, followed by Tukey's honest significant difference (HSD) multiple pairwise comparisons

gene expression of *hgf* with both SR- and RR-RvD6 cornea treatments (Figure 5C).

## 4 | DISCUSSION

Previous studies from our laboratory have demonstrated that PEDF + DHA treatment decreases inflammation and increases wound healing and nerve regeneration using different models of corneal injuries and infection.[16-19] The mechanism involves the phospholipase A2 activity of the PEDF receptor that releases DHA incorporated in the membrane phospholipids and leads to the synthesis of docosanoids.[15] By LC-MS/MS isolation and fragmentation analysis, we identify one of the docosanoids release in tears as an RvD6 isomer with a retention time different than the RvD6 standard with *SS*-configuration.[21] The new isomer enhances corneal wound healing, increased recovery of sensitivity, and activates nerve regeneration.[21]

Here, we showed that RvD6si release to the media from injured corneas stimulated by PEDF + DHA were significantly inhibited by Fluvoxamine, an inhibitor of cytochrome P450, but not by 15-LOX or 5-LOX inhibitors. These data suggested that there is a 17*R*-monohydroxy group in the DHA derivative. Therefore, the chemical synthesis of 4*R*-17*R*-dihydroxy-DHA (RR-RvD6) and 4*S*-17*R*-dihydroxy-DHA (SR-RvD6) was performed in order to confirm the isomer structure. Using an innovative method, we obtained these two molecules with more than 90% purity (Figure 2B), which by chiral separation, provided two matched peaks to our RvD6si isolated from mouse tears (Figure 2C).

Our experiments demonstrate that 5-LOX inhibitors and antibodies did not show a decrease in the synthesis of RvD6si. Therefore, we do not have a satisfactory explanation for how the synthesis of SR-RvD6i occurs. One possibility is that the inhibitors were not specific enough to block the synthesis of this isomer. Alternatively, the isomer is produced by a pathway that does not include 5-LOX. Further studies will be needed to determine the origin of SR-RvD6 in tears after injury. When the biological activities of RR-RvD6 and SR-RvD6 on corneal sensation and nerve recovery were assessed, we found that RR-RvD6 was the only isomer that increased the sensitivity 3 days after injury, suggesting that this lipid mediator has a higher potency than SR- and SS-RvD6 isomers. Moreover, the percentage of total corneal nerve recovery and the SP-positive nerves in the RR-RvD6 group were even higher than in the PEDF + DHA-treated group (Figure 3). The results demonstrate that the RR-RvD6 isomer has a stronger effect on corneal nerve regeneration than the mixture of isomers obtained after PEDF + DHA treatment. Even though PEDF + DHA was applied in the same manner (three times per day for 12 days), the higher efficiency of RR-RvD6 could be caused by its defined structure and higher molarity since the conversation of PEDF + DHA to RvD6si is low. For this reason, the administration of 1 ng/μL of RR-RvD6 is much higher than the actual amount synthesized by PEDF + DHA in vivo.

One of the advantages of RvD6si treatment was pain management.[21] Unlike other ongoing therapies, such as NGF,[38] RvD6si provided an alternative way to increase corneal nerve density without stimulating the expression of genes associated with pain in the TG. Using RNA-seq analysis of the homolateral TG, we show that both RR-RvD6- and SR-RvD6-treated mice show a significantly lower gene expression than the vehicle of genes encoding pain-related neuropeptides, such as SP and CGRP while *Trpm8*, the transient channel that diminished in dry eye-like pain conditions,[36,37,39,40] was significantly elevated in SR- and RR-RvD6-treated corneas than vehicle and SS-RvD6-treated groups (Figure 4B). Tac1 encodes SP, one of the most abundant neuropeptides expressed in corneal nerves[25-27] that causes pro-inflammatory effects and clinical chronic pain[41] while Calcb encodes CGRP, another abundant neuropeptide[42] that plays an essential role in neurogenic inflammation and pain.[43] The inhibition of these neuropeptides in the TG suggests successful management of potential neuropathic pain by treatment with RR-RvD6 and SR-RvD6. Future studies to further investigate the action of the new lipids in models of corneal pain will be needed. In addition, the topical application of these lipid mediators increases corneal nerve outgrowth by fostering the Rictor-related signaling as well as other neurotrophic genes. Due to the important role of Rictor in downregulated several genes in the TG, we discovered an important role of Rictor in decreasing the induction of genes involved in degenerative diseases using the KEGG pathway enrichment analysis. It will be important to investigate the role of Rictor in models of brain diseases.

Our RNA-seq data also shows a significant increase in the expression of *Hgf*, which encodes HGF, a paracrine growth factor that is expressed in corneal stroma and stimulates

epithelial proliferation and suppresses inflammation after injury through its receptor Met tyrosine kinase.[44-46] IPA predicts that RR-RvD6 activates a group of axonal outgrowth genes in the TG involved in neuritogenesis and branching of neurites, which are important to regenerate corneal nerves, with HGF being a central factor in these biological functions

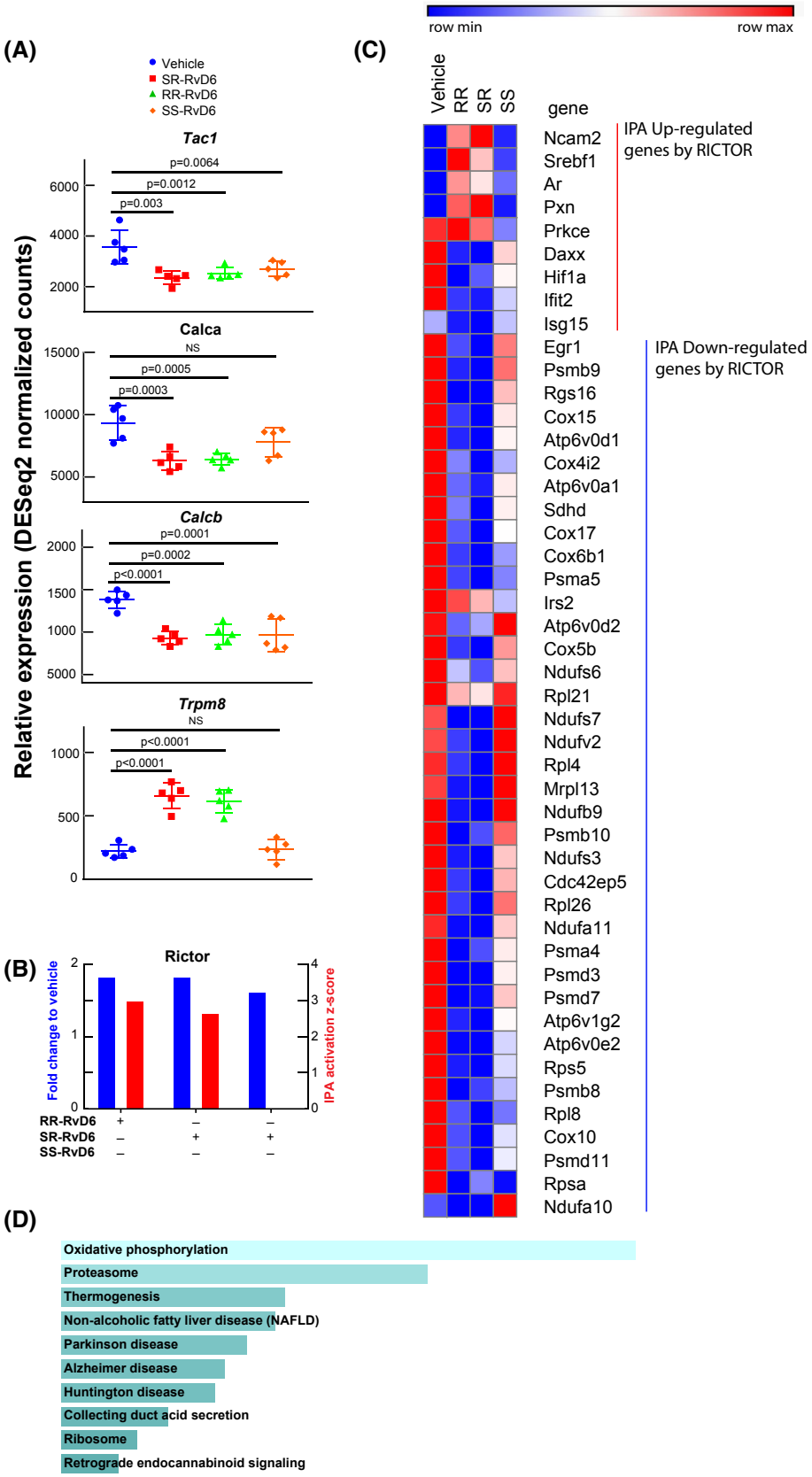

**FIGURE 4** Transcriptome signature in the trigeminal ganglion unravels the role of RvD6 isomers. A, RNA-seq normalized counts of genes involved in inflammation and pain, including *Tac1*, *Calca*, *Calcb*, and *Trpm8*. The *p* values are derived from ANOVA post hoc Dunnett's multiple comparisons test with vehicle as a reference. Mean and SD are depicted as the lines. Each data point represents an ipsilateral TG of a mouse. B, The *Rictor* signaling activated by RvD6 isomers. The blue columns represent the relative normalized fold changes of *Rictor* gene analyzed by RNA-seq, while the red columns represent the activation z-score of *Rictor* signaling predicted by IPA using RNA-seq data as input. The SS-RvD6 z-score was insufficient to show the activation of RICTOR pathway in the IPA. C, The RNA-seq normalized counts heatmap of RICTOR regulated genes. The genes activated (red) and inhibited (blue) are grouped and clustered across all treatment groups. There are about 5 upregulated genes and 36 downregulated genes by SR-and RR-RvD6. D, The KEGG-pathway prediction of RICTOR downregulated genes from C. Bars were sorted by *p* value. The length of the bar represents the significance of the pathway, while the lighter the color, the higher the significance

**FIGURE 5** Predicted action of RR-RvD6 on nerve growth in the trigeminal ganglia. A, The IPA of nervous system development and functions in the TG after RR-RvD6-treated corneas in mice. The bar chart shows the activation z-score (blue) and *p* value (red) of 12 significant groups of biological functions. B, The graphical summary of RR-RvD6 induced axon regeneration with *hgf* expression as a central upstream modulator. Dash lines represent that *Hgf* requires several intermediate signaling pathways to reach the biological function. C, Hgf was found significantly elevated by *SR*- and *RR*-RvD6 treatment but not by *SS*-RvD6

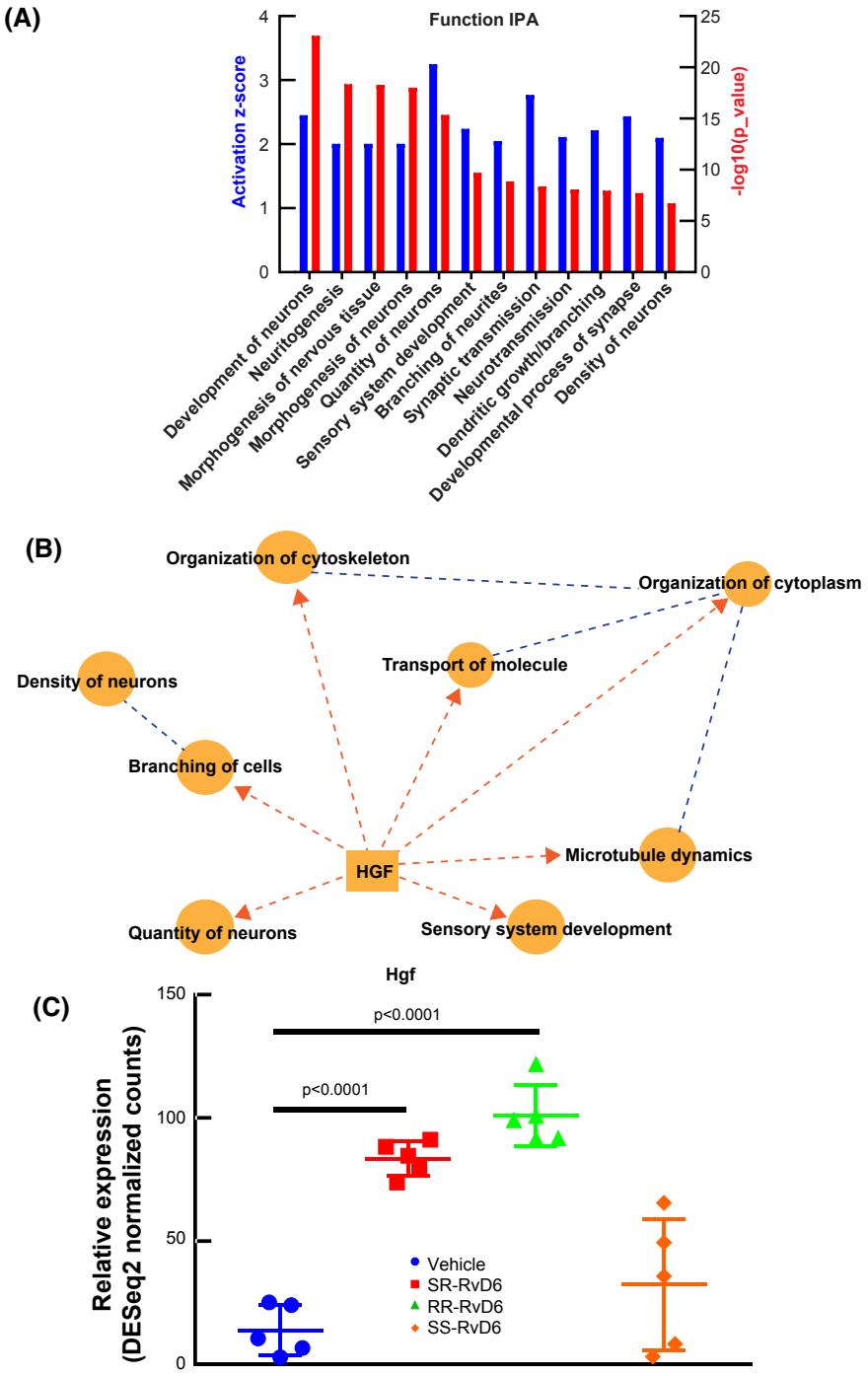

(Figure 5). Previous studies have shown that HGF signaling enhances axonal growth of periphery sensory neurons from the skin in a mice model[47] and increases peripheral nerve regulation after sciatic nerve injury.[48] It is interesting that cornea nerves can transmit signals to the TG,[49] but further studies will be needed to decode the working mechanism of RR-RvD6 on the cornea-TG axis, especially how topical treatment with RR-RvD6 can affect the cornea-innervating neuron in the TG as well as how RR-RvD6 stimulated corneal epithelial cells can interact with corneal nerve axons to enhance nerve recovery.

Recently, in an alkali burn rat model as well as in human corneal epithelial cells in culture challenged with IFNγ, we found that treatment with RR-RvD6 decreases inflammation, cytokine expression, and senescence programming, demonstrating the protective bioactivity of this lipid.[50] Interestingly, RR-RvD6 decreases the expression of ACE2, the receptor of coronavirus SARS-CoV-2, and the binding of the receptor-binding domain (RBD) of the virus spike protein to ACE2. The data suggest that RR-RvD6 may have therapeutic value in decreasing the damage produced by this viral infection.

In conclusion, this study uncovers the stereochemical structure of RvD6si released from tears in a mouse injury model as a mixture of four isomers, with 4*R*-17*R*-dihydroxy-DHA being a more biologically potent isomer than the mixture obtained after PEDF + DHA treatment. In addition, *RR*-RvD6 stimulates a specific transcriptome in the TG with *Rictor* and *hgf* as key regulators to modulate axonal growth and decrease pain, which is not reported by other docosanoids.[51-55]

## ACKNOWLEDGMENTS

The authors are grateful to Drs. Jovanny Zabaleta and Jone Garai [Louisiana Cancer Research Center Translational Genomics Core] for the sequencing. This work was supported by the National Institutes of Health/National Eye Institute Grant R01EY019465 (to HEPB).

## CONFLICT OF INTEREST

The subject matter of this manuscript is protected by a US provisional patent application assigned to the Board of Supervisors of Louisiana State University and Agricultural and Mechanical College (LSU) and licensed to a company, CurVirBiotech, founded by co-author Nicolas G. Bazan.

## AUTHOR CONTRIBUTIONS

H. E. P. Bazan and T. L. Pham designed the experiments. T. L. Pham performed acquisition and analysis of the data, and writing and critical review of the manuscript; A. H. Kakazu coded and prepared the drugs, performed lipid extraction, and helped with RNA extraction and sensitivity measurement. J. He did the injury, treatments, and isolation of corneal tissues. R. Nshimiyimana and N. A. Petasis synthesized RR- and SR-RvD6i. B. Jun performed the LC-MS/MS lipid analysis and acquisition of data. J. He, A. H. Kakazu, and B. Jun provided a critical review of the manuscript. N. G. Bazan contributed to the interpretation of results and reviewed the manuscript. H. E. P. Bazan supervised the study, wrote and reviewed the manuscript, and was responsible for the integrity of this work.

## REFERENCES

1. Müller LJ, Marfurt CF, Kruse F, Tervo TMT. Corneal nerves: structure, contents and function. *Exp Eye Res*. 2003;76(5):521-542.
2. He J, Bazan HEP. Mapping the nerve architecture of diabetic human corneas. *Ophthalmology*. 2012;119(5):956-964. https://doi.org/10.1016/j.ophtha.2011.10.036
3. Hamrah P, Cruzat A, Dastjerdi MH, et al. Corneal sensation and subbasal nerve alterations in patients with herpes simplex keratitis: an in vivo confocal microscopy study. *Ophthalmology*. 2010;117(10):1930-1936. https://doi.org/10.1016/j.ophtha.2010.07.010
4. Cruzat A, Witkin D, Baniasadi N, et al. Inflammation and the nervous system: the connection in the cornea in patients with infectious keratitis. *Invest Ophthalmol Vis Sci*. 2011;52(8):5136-5143. https://doi.org/10.1167/iovs.10-7048
5. He J, Bazan HEP. Corneal nerve architecture in a donor with unilateral epithelial basement membrane dystrophy. *Ophthalmic Res*. 2013;49(4):185-191. https://doi.org/10.1159/000345766
6. He J, Bazan NG, Bazan HEP. Mapping the entire human corneal nerve architecture. *Exp Eye Res*. 2010;91(4):513-523. https://doi.org/10.1016/j.exer.2010.07.007
7. Erie JC, McLaren JW, Hodge DO, Bourne WM. Recovery of corneal subbasal nerve density after PRK and LASIK. *Am J Ophthalmol*. 2005;140(6):1059-1064. https://doi.org/10.1016/j.ajo.2005.07.027
8. Chao C, Golebiowski B, Stapleton F. The role of corneal innervation in LASIK-induced neuropathic dry eye. *Ocul Surf*. 2014;12(1):32-45. https://doi.org/10.1016/j.jtos.2013.09.001
9. Linna TU, Vesaluoma MH, Pérez-Santonja JJ, Petroll WM, Alió JL, Tervo TM. Effect of myopic LASIK on corneal sensitivity and morphology of subbasal nerves. *Invest Ophthalmol Vis Sci*. 2000;41(2):393-397.
10. Kymionis GD, Grentzelos MA, Kalyvianaki MI, et al. Fifteen-year follow-up after anterior chamber phakic intraocular lens implantation in one and LASIK in the fellow eye. *Semin Ophthalmol*. 2009;24(6):231-233. https://doi.org/10.3109/08820530903388751
11. Lee BH, McLaren JW, Erie JC, Hodge DO, Bourne WM. Reinnervation in the cornea after LASIK. *Invest Ophthalmol Vis Sci*. 2002;43(12):3660-3664.
12. Hovanesian JA, Shah SS, Maloney RK. Symptoms of dry eye and recurrent erosion syndrome after refractive surgery. *J Cataract Refract Surg*. 2001;27(4):577-584.
13. Rosenthal P, Borsook D. Ocular neuropathic pain. *Br J Ophthalmol*. 2016;100(1):128-134. https://doi.org/10.1136/bjophthalmol-2014-306280
14. Pham TL, Bazan HEP. Docosanoid signaling modulates corneal nerve regeneration: effect on tear secretion, wound healing, and neuropathic pain. *J Lipid Res*. 2021;62:100033. https://doi.org/10.1194/jlr.TR120000954
15. Pham TL, He J, Kakazu AH, Jun B, Bazan NG, Bazan HEP. Defining a mechanistic link between pigment epithelium-derived

factor, docosahexaenoic acid, and corneal nerve regeneration. *J Biol Chem*. 2017;292(45):18486-18499. https://doi.org/10.1074/jbc.M117.801472

16. Cortina MS, He J, Li N, Bazan NG, Bazan HEP. Neuroprotectin D1 synthesis and corneal nerve regeneration after experimental surgery and treatment with PEDF plus DHA. *Invest Ophthalmol Vis Sci*. 2010;51(2):804-810. https://doi.org/10.1167/iovs.09-3641
17. Cortina MS, He J, Russ T, Bazan NG, Bazan HEP. Neuroprotectin D1 restores corneal nerve integrity and function after damage from experimental surgery. *Invest Ophthalmol Vis Sci*. 2013;54(6):4109-4116. https://doi.org/10.1167/iovs.13-12075
18. He J, Cortina MS, Kakazu A, Bazan HEP. The PEDF neuroprotective domain plus DHA induces corneal nerve regeneration after experimental surgery. *Invest Ophthalmol Vis Sci*. 2015;56(6):3505-3513. https://doi.org/10.1167/iovs.15-16755
19. He J, Neumann D, Kakazu A, et al. PEDF plus DHA modulate inflammation and stimulate nerve regeneration after HSV-1 infection. *Exp Eye Res*. 2017;161:153-162. https://doi.org/10.1016/j.exer.2017.06.015
20. He J, Pham TL, Kakazu A, Bazan HEP. Recovery of corneal sensitivity and increase in nerve density and wound healing in diabetic mice after PEDF plus DHA treatment. *Diabetes*. 2017;66(9):2511-2520. https://doi.org/10.2337/db17-0249
21. Pham TL, Kakazu AH, He J, Jun B, Bazan NG, Bazan HEP. Novel RvD6 stereoisomer induces corneal nerve regeneration and wound healing post-injury by modulating trigeminal transcriptomic signature. *Sci Rep*. 2020;10(1):4582. https://doi.org/10.1038/s41598-020-61390-8
22. Bligh EG, Dyer WJ. A rapid method of total lipid extraction and purification. *Can J Biochem Physiol*. 1959;37(8):911-917. https://doi.org/10.1139/o59-099
23. Belmonte C, Acosta MC, Schmelz M, Gallar J. Measurement of corneal sensitivity to mechanical and chemical stimulation with a $CO_2$ esthesiometer. *Invest Ophthalmol Vis Sci*. 1999;40(2):513-519.
24. Murphy PJ, Lawrenson JG, Patel S, Marshall J. Reliability of the non-contact corneal aesthesiometer and its comparison with the Cochet-Bonnet aesthesiometer. *Ophthalmic Physiol Opt J Br Coll Ophthalmic Opt Optom*. 1998;18(6):532-539.
25. He J, Bazan HEP. Neuroanatomy and neurochemistry of mouse cornea. *Invest Ophthalmol Vis Sci*. 2016;57(2):664-674. https://doi.org/10.1167/iovs.15-18019
26. He J, Pham TL, Bazan HEP. Mapping the entire nerve architecture of the cat cornea. *Vet Ophthalmol*. 2019;22(3):345-352. https://doi.org/10.1111/vop.12600
27. He J, Pham TL, Bazan HEP. Neuroanatomy and neurochemistry of rat cornea: Changes with age. *Ocul Surf*. 2020;20:86-94. https://doi.org/10.1016/j.jtos.2020.11.005
28. Pham TL, Kakazu A, He J, Bazan HEP. Mouse strains and sexual divergence in corneal innervation and nerve regeneration. *FASEB J*. 2019;33(3):4598-4609. https://doi.org/10.1096/fj.201801957R
29. Picelli S, Faridani OR, Björklund AK, Winberg G, Sagasser S, Sandberg R. Full-length RNA-seq from single cells using Smart-seq2. *Nat Protoc*. 2014;9(1):171-181. https://doi.org/10.1038/nprot.2014.006
30. Liao Y, Smyth GK, Shi W. The R package Rsubread is easier, faster, cheaper and better for alignment and quantification of RNA sequencing reads. *Nucleic Acids Res*. 2019;47(8):e47. https://doi.org/10.1093/nar/gkz114
31. Liao Y, Smyth GK, Shi W. featureCounts: an efficient general purpose program for assigning sequence reads to genomic features. *Bioinforma Oxf Engl*. 2014;30(7):923-930. https://doi.org/10.1093/bioinformatics/btt656
32. Love MI, Huber W, Anders S. Moderated estimation of fold change and dispersion for RNA-seq data with DESeq2. *Genome Biol*. 2014;15(12):550. https://doi.org/10.1186/s13059-014-0550-8
33. Kuleshov MV, Jones MR, Rouillard AD, et al. Enrichr: a comprehensive gene set enrichment analysis web server 2016 update. *Nucleic Acids Res*. 2016;44(W1):W90-97. https://doi.org/10.1093/nar/gkw377
34. Zeldin DC. Epoxygenase pathways of arachidonic acid metabolism. *J Biol Chem*. 2001;276(39):36059-36062. https://doi.org/10.1074/jbc.R100030200
35. Serhan CN, Hong S, Gronert K, et al. Resolvins: a family of bioactive products of omega-3 fatty acid transformation circuits initiated by aspirin treatment that counter proinflammation signals. *J Exp Med*. 2002;196(8):1025-1037. https://doi.org/10.1084/jem.20020760
36. He J, Pham TL, Kakazu AH, Bazan HEP. Remodeling of substance P sensory nerves and transient receptor potential melastatin 8 (TRPM8) cold receptors after corneal experimental surgery. *Invest Ophthalmol Vis Sci*. 2019;60(7):2449-2460. https://doi.org/10.1167/iovs.18-26384
37. Liu B, Fan L, Balakrishna S, Sui A, Morris JB, Jordt S-E. TRPM8 is the principal mediator of menthol-induced analgesia of acute and inflammatory pain. *Pain*. 2013;154(10):2169-2177. https://doi.org/10.1016/j.pain.2013.06.043
38. Bonini S, Lambiase A, Rama P, Caprioglio G, Aloe L. Topical treatment with nerve growth factor for neurotrophic keratitis. *Ophthalmology*. 2000;107(7):1347-1351; discussion 1351–1352. https://doi.org/10.1016/s0161-6420(00)00163-9
39. Parra A, Madrid R, Echevarria D, et al. Ocular surface wetness is regulated by TRPM8-dependent cold thermoreceptors of the cornea. *Nat Med*. 2010;16(12):1396-1399. https://doi.org/10.1038/nm.2264
40. Belmonte C, Gallar J. Cold thermoreceptors, unexpected players in tear production and ocular dryness sensations. *Invest Ophthalmol Vis Sci*. 2011;52(6):3888-3892. https://doi.org/10.1167/iovs.09-5119
41. Zieglgänsberger W. Substance P and pain chronicity. *Cell Tissue Res*. 2019;375(1):227-241. https://doi.org/10.1007/s00441-018-2922-y
42. Cortina MS, He J, Li N, Bazan NG, Bazan HEP. Recovery of corneal sensitivity, calcitonin gene-related peptide-positive nerves, and increased wound healing induced by pigment epithelial-derived factor plus docosahexaenoic acid after experimental surgery. *Arch Ophthalmol Chic Ill 1960*. 2012;130(1):76-83. https://doi.org/10.1001/archophthalmol.2011.287
43. Iyengar S, Ossipov MH, Johnson KW. The role of calcitonin gene–related peptide in peripheral and central pain mechanisms including migraine. *Pain*. 2017;158(4):543-559. https://doi.org/10.1097/j.pain.0000000000000831
44. Wilson SE, Liu JJ, Mohan RR. Stromal-epithelial interactions in the cornea. *Prog Retin Eye Res*. 1999;18(3):293-309. https://doi.org/10.1016/s1350-9462(98)00017-2
45. Chandrasekher G, Pothula S, Maharaj G, Bazan HEP. Differential effects of hepatocyte growth factor and keratinocyte growth factor on corneal epithelial cell cycle protein expression, cell survival, and growth. *Mol Vis*. 2014;20:24-37.
46. Omoto M, Suri K, Amouzegar A, et al. Hepatocyte growth factor suppresses inflammation and promotes epithelium repair in corneal injury. *Mol Ther J Am Soc Gene Ther*. 2017;25(8):1881-1888. https://doi.org/10.1016/j.ymthe.2017.04.020

47. Maina F, Hilton MC, Ponzetto C, Davies AM, Klein R. Met receptor signaling is required for sensory nerve development and HGF promotes axonal growth and survival of sensory neurons. *Genes Dev*. 1997;11(24):3341-3350. https://doi.org/10.1101/gad.11.24.3341
48. Ko KR, Lee J, Lee D, Nho B, Kim S. Hepatocyte Growth Factor (HGF) promotes peripheral nerve regeneration by activating repair Schwann cells. *Sci Rep*. 2018;8(1):8316. https://doi.org/10.1038/s41598-018-26704-x
49. Ferrari G, Bignami F, Giacomini C, et al. Ocular surface injury induces inflammation in the brain. in vivo and ex vivo evidence of a corneal-trigeminal axis. *Invest Ophthalmol Vis Sci*. 2014;55(10):6289-6300. https://doi.org/10.1167/iovs.14-13984
50. Pham TL, He J, Kakazu AH, et al. Elovanoid-N32 or RvD6-isomer decrease ACE2 and binding of S protein RBD after injury or INFγ in the eye. *Res Sq*. Published online August 11, 2020. 10.21203/rs.3.rs-55764/v1
51. Gronert K, Maheshwari N, Khan N, Hassan IR, Dunn M, Schwartzman ML. A role for the mouse 12/15-lipoxygenase pathway in promoting epithelial wound healing and host defense. *J Biol Chem*. 2005;280(15):15267-15278. https://doi.org/10.1074/jbc.M410638200
52. Jin Y, Arita M, Zhang Q, et al. Anti-angiogenesis effect of the novel anti-inflammatory and pro-resolving lipid mediators. *Invest Ophthalmol Vis Sci*. 2009;50(10):4743-4752. https://doi.org/10.1167/iovs.08-2462
53. Hua J, Jin Y, Chen Y, et al. The resolvin D1 analogue controls maturation of dendritic cells and suppresses alloimmunity in corneal transplantation. *Invest Ophthalmol Vis Sci*. 2014;55(9):5944-5951. https://doi.org/10.1167/iovs.14-14356
54. Obrosov A, Coppey LJ, Shevalye H, Yorek MA. Effect of fish oil vs. resolvin D1, E1, methyl esters of resolvins D1 or D2 on diabetic peripheral neuropathy. *J Neurol Neurophysiol*. 2017;8(6): https://doi.org/10.4172/2155-9562.1000453
55. Zhang Z, Hu X, Qi X, et al. Resolvin D1 promotes corneal epithelial wound healing and restoration of mechanical sensation in diabetic mice. *Mol Vis*. 2018;24:274-285.

**How to cite this article:** Pham TL, Kakazu AH, He J, et al. Elucidating the structure and functions of Resolvin D6 isomers on nerve regeneration with a distinctive trigeminal transcriptome. *The FASEB Journal*. 2021;35:e21775. https://doi.org/10.1096/fj.202100686R